Jurnal Kejuruteraan 32(3) 2020: 357-371
https://doi.org/10.17576/jkukm-2020-32(3)-01

Recent Applications of Residual Stress Measurement Techniques for FSW Joints: A Review

Mustafa Ali A. Glaissa, Mohammed Asmael*& Qasim. Zeeshan
[a]*Department of Mechanical Engineering, Eastern Mediterranean University, Famagusta, North Cyprus, Via Mersin 10, Turkey*

**Corresponding author: mohammed.asmael@emu.edu.tr*

Received 25 September 2018, Received in revised form 24 June 2019
Accepted 23 September 2019, Available online 30 August 2020

ABSTRACT

Quality control of welding processes plays a significant role in characterizing of the weld quality. Various Non-Destructive Method (NDM), Semi-Destructive Method (SDM) and Destructive Method (DM) are all employed for welding inspection and quality control. This paper presents a review of the recent research onthe quality control of Friction Stir Welding (FSW) processes of similar and dissimilar alloys. Based on previews articles, this paper focuses on comparing various inspection techniques with the effect of different FSW parameters such as; tilt angle (deg°), rotation speed (rpm), welding speed (mm/min) and axial applied force (N)on the formation or residual stresses across welded joints. Additionally, the inspection measuring parameters, machine used, and material specification are also discussed. Recent studies are classified based on the measuring approach. The key findings for each inspection method are also presented. Researchers report that NDM, SMD and DM greatly contribute in detecting residual stresses of welded joints. However, some techniques like Deep-hole drilling technique have not been extensively applied for quality inspection of the FSW process. This paper reviews the various testing techniques for the FSW, aiming to let more experts know the current research status and also provide some guidance for future research.

Keywords: Friction stir welding; non-destructive methods; semi-destructive methods; destructive methods; residual stresses

INTRODUCTION

AFriction Stir Welding (FSW)invented in England, U.K. at The Welding Institute (TWI) By Wayne Thomas in 1991 (Sidhu and Chatha 2012), is a solid state welding process that joins similar and dissimilar metals that are not able to be welded by means of fusion processes. FSW process principle is based on using friction force in order to join adjacent metals surfaces without reaching the melting point of the welded materials. FSW process is highly desired in the aerospace field as it can weld mostly all types of aluminum alloys. This process can produce fumes-free, crack-free and high quality joints. FSW process softens the adjacent materials by utilizing a rotating profiled tool that plunges into a certain depth in metal(Thomas et al. 2009). Figure 1 illustrates schematically the principle of FSW process.

Additionally, FSW is capable to weld metals which they are difficult to weld by fusion-state welding process at low energy consumption rate, such as; steel (Wei and Nelson 2011), titanium(Dressler et al. 2009; Thomas 2003) and composites matrices (Uzun2007; Chen 2009). It is important to choose the proper welding parameters; tool speed, weld speed, tilt angle, and dwell time in order to achieve high quality FSWed joint. Furthermore, tool material and tool pin profile are key elements to improve the mechanical and microstructural properties of the welded joint (Al-Moussawi and Smith 2018). However, welding defects such as residual stresses (RS) are unavoidable in post-welding in both solid and fusion state welding processes (Singh 2012). This paper reviews recent researches on quality control technologies of FSW procescs.

WELD QUALITY STANDARD

The weld quality expresses the welded joints capability to carry out the feasible requirements of the weld during the life-cycle of the structure. This gives the possibility be either durability in dynamic and/or static loading, corrosion resistance, shape, or any other mechanical functions.Deficient in quality has to be avoided due to the severe consequences in cost and safety, i.e., failure take place at an early stage. Excessive quality .however, might outcome in increased machining cost which does not add more value to the product. Furthermore, it is compulsory as a design engineer to identify the sufficient quality in the linked locations of the structure, as different locations in the structure might experience excessive loading due to local stress raisers such as holes, stiffeners and notches (Barsoum et al. 2012).Generally, inspection of welds quality is classified according to the three main quality levels; A, B and C. Where, level of quality A denotes for the highest finished weld requirements which its failure would cause

severe danger to welder.Class B corresponds to semi-critical application. Thus, its failure would reduce the strength of used equipment or system. Class B represents non-critical application that has no effect in the system in case of failure (Ding 2008).

Standard D17.3M:2010 has lately been published by American Welding Society (AWS) and reports the 'Specification of FSW of Aluminum Alloys for Aerospace Industry'. This standard covers; joint weld design, procedure and qualification development of FSW process. Additionally, fabrication guidance such as pre-weld joint preparation, FSW tool and post-weld preparation of service were also reported (Stenberg et al. 2017).Table 1 shows a number of recent FSW process standards developed by different welding organizations.

RESIDUAL STRESSES

While it is not the main aim to review the types of residual stress in detail. However, it is significant to consider briefly the effects of RS on welding quality as it is consider as one of major causes to welding defects according to American Society of Mechanical Engineers (ASME). When a material is subjected to machining or heat treatment processing, internal stresses are arise. Compressive stress ($\sigma_{s,+}$) and tensile stress ($\sigma_{t,}$ -) denoting the residual stresses components. A significant cause of RS is welding process, as shown in Figure 2, regions (1-4), the contraction behavior of the moltenmetal(region 2)induces longitudinal and transverse residual stresses at region 1 and 3 respectively, during cooling emerging of RS due to the resistance of the cold base metal. Consequently, distortion of metal accrued at region 4 due to internal compressive and tensile stresses(Suominen et al. 2013).However, annealing stress relief can eliminate these stresses(Noyanand Cohen2013). RS can be classified into type 1 macrostresses that can arise due differing constantly over large distances, type 2 intergranular or microscopic stresses, that vary within the material's grain and type 3 atomic scale stresses (Withers and Bhadeshia 2001). Figure 3 and 4 show type 1 & 2 RS respectively, where ***α and*** β denote formultiphase material with internal microstresses ***(σ)***. However,the effect of residual stresses can have positive or negative effect, based on the signs, magnitude, and distribution of the stresses over weld and base regions. Excessive applied tensile stress near material's surface can play major role in crack initiation. Shot peening is useful to overcome these RS. This cold working process impacts the material's surface by using small rounded abrasives in order to produce compressive residual stress (CRS) to balance the interior tensile RS (Macherauch and Wohlfahrt 1978). The magnitudes of those numerous types of stresses may be have a big portion (half or more) of the UTS of the annealed material (Macherauch 1987).

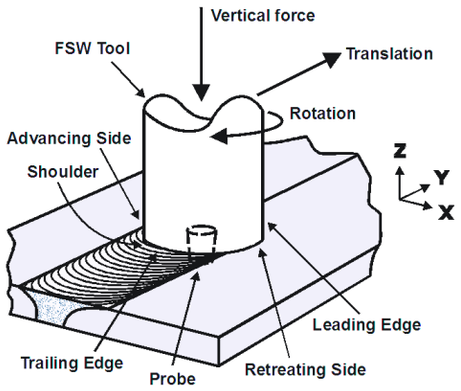

FIGURE 1. FSW process. Adapted from (Jata et al. 2000)

TABLE 1. FSW standards

No.	Standard Number	Standard Title	Institute/society
1	ISO 25239-1:2011	FSW -- Aluminum -- Part 1: Vocabulary	International Institute of Welding (IIW)
2	ISO 25239-2:2011	FSW -- Aluminum -- Part 2: Design of weld joints	
3	ISO 25239-3:2011	FSW -- Aluminum -- Part 3: Qualification of welding operators	
4	ISO 25239-4:2011	FSW -- Aluminum -- Part 4: Specification and qualification of welding procedures	
5	ISO 25239-5:2011	FSW -- Aluminum -- Part 5: Quality and inspection requirements	
6	ISO 15620:2000	Friction welding of metallic materials	Foreign Direct Investment (FDI)
7	D17.3/D17.3M:2010	Specification for Friction Stir Welding of Aluminum Alloys for Aerospace Applications	American Welding Society (AWS)

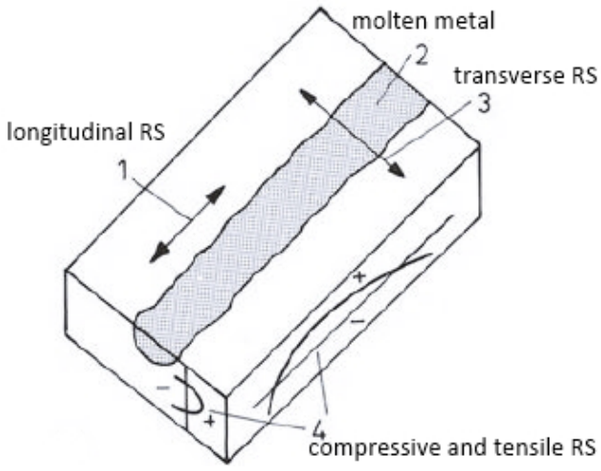

FIGURE 2.Residual stress due to welding. Adapted from (Noyan and Cohen 2013)

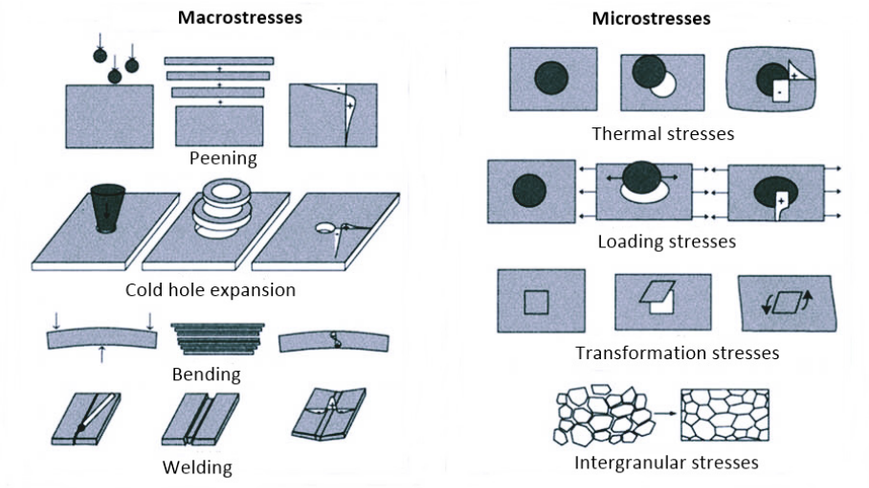

FIGURE 3. Type 1 and 2 residual stresses. Adapted from (Hutchings et al. 2005)

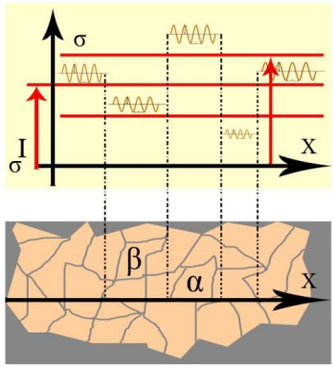

FIGURE 4. Type 3 residual stress. Adapted from (Hutchings et al. 2005)

INSPECTION METHODS

In order to measure and control residual stresses in Weldments, scientists have developed and applied various inspection methods over the years. These quality control testing methods can be classified as; (Destructive, Semi Destructive and Non Destructive) methods. Relaxing methods are based on analyzing the distorted parts by removing certain region from the weldment's material. The removed material induces stress-relaxation that can be

measured by using electrical-strain gages to examine the weld quality. Slitting, contour, hole-drilling, ring-core, and deep-hole techniques are the classified under destructive and semi-destructive methods. Nondestructive methods include; x-ray, neutron diffraction, ultrasonic, and magnetic technics.

Quality inspection methods frequently measure certain parameter that is linked to the arise stresses, i.e. wave length λ and stress directions within lattice planes using x-ray technique, For investigating fatigue-related destruction, and they come to be even more important since several structural components, e.g., bridges constructions, airplane structures, or off-shore platforms, need to be periodically inspected to prevent major damage or even failure. For inspection in the work field or on large scale constructions, small components, and easy-to-carry devices are significant (Benyounis et al. 2014). Moreover, NDM are cost-effective and requires less measuring time in preparation of the part prior to the test (Chang 1999). Figure 5 shows the three major classifications of NDM schematically.

NON-DESTRUCTIVE METHODS (NDM)

NDT methods are trying out or investigating materials, components or assemblies for discontinuities, or variations in characteristics without destroying the serviceability of the component or device. In other phrases, whilst the inspection or check is completed the element can nonetheless be used.

DIFFRACTION TECHNIQUES

These types of techniques are used to obtain the elastic deformation within atomic lattice spacing, d, from the stress-free value, d_0 of the lattice that causes interplanar spacing, d.

X-RAY DIFFRACTION TECHNIQUE

Based on Bragg's law, (Cole 1970) the diffracted ray triggered to the crystal atoms is calculated by the given equation (1) as;

$$2d \sin\theta = n\lambda \quad (1)$$

Where, λ is the wave length, d is the lattice interplanar spacing, is a positive integer and n represents the maximum diffraction angle. In a crystal lattice atoms are arranged as shown in Figure 6, thus the separation distance in in order of the wave length of the triggered ray. Assuming that x-ray is directed at the crystal lattice, so two incidents rays are parallel to one another making an angle θ with respect to plane of lattice (Pope 1997).The x-ray technique is classified under nondestructive methods for the measurement of residual stresses into a certain depth of material surfaces. X-ray diffraction techniques principle is based on Bragg's law used for defining materials using x-rays which have very short wavelengths on the scale of an angstrom. X-ray passes though slits that reduce the angular divergence to keep it on the right path to hit the atoms in sample with angle, as shown in Figure 6, the path of the x-ray is diffracted and received by the detector at angle of 2. RS causes spacing of grains planes parallel to the grain planes of surface at some position of sample. Consequently, the x-ray will diffract proportional to the peak intensity as shown in Figure 7. However, plane spacing values will act as strain gauge that measures RS of macro and micro scales (Warren 1969). In order to find the strain, $\boldsymbol{\varepsilon}$ for plane spacing, d expressed by equation (2) as;

$$\boldsymbol{\varepsilon} = \frac{\Delta d}{d} \quad (2)$$

And thus, the strain value is equal to the partial derivative of equation 1.1(Kaniowski et al. 2011) with respect to plane spacing, d gives by equation (3);

$$\boldsymbol{\varepsilon} = -\delta\theta \cot\theta \quad (3)$$

Mokabberi et al. (2018) have studied the effect of interlayers of copper, zinc and brass on microstructural and mechanical properties of FSWed AA 1050 aluminum alloy. The X-ray spectroscopy (EDS) technique was utilized to inspect the

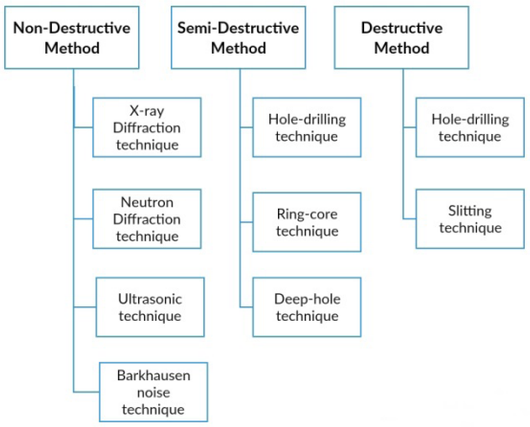

FIGURE 5. Classifications of NDM, SMD and DM (Büyüköztürk and Taşdemir 2012)

characteristics of the different regions of the weld and to study effect of the interlayers on grains structure in the SZ. Results have shown that welding without using interlayers; the joint efficiency was approximately 60%. While the brass interlayer has improved joint seam efficiency up to ~90% .However, copper and zinc interlayers had no significant effect on the seam joint efficiency. Prasad et al. (2018) have considered welding parameters effect of joining AZ91 Mg alloy with AA 6063 aluminum alloy sheets by FSW process. A successful joint was accomplished at tool rotation speed of 1100 rpm and welding speed of 25 mm/min tool. By using X-ray diffraction analysis it can be understood that the joining of AZ91 Mg alloy with Al6063 alloy can be achieved by FSW and No important different phases were found based on XRD results. Nevertheless, (Carlone and Palazzo 2015) have characterized butt -joint quality of cast ZE41A Mgalloy welded by both FSW and TIG processes. X-ray (GILARDONI AION160) device was utilized to detect longitudinal residual stresses (LRS) formed in the butt-joint configuration. Authors have reported that LRS induced by TIG process were higher than FSW process. In addition, (Commin et al. 2012) have studied the effect of FSW process on microstructure evolution, mechanical properties and RS of AZ31 hot-rolled sheets. FSWed joint was inspected utilizing SEIFRT MZ6TS diffractometer. As results, high tensile RS were detected in TMAZ, with large concentration at advancing side. Furthermore, the resulting RS induced by FSW were large comparing to the yield strength value of base metal.

NEUTRON DIFFRACTION TECHNIQUE

Neutron diffraction technique is similar x-ray technique in terms of applying measuring mechanism. However, this technique utilizes proton beam which hits and penetrate a target and then becomes excited, the protons are splits into a process known as (spallation) and emits neutrons. The detector receives the diffracted neutron beam at certain

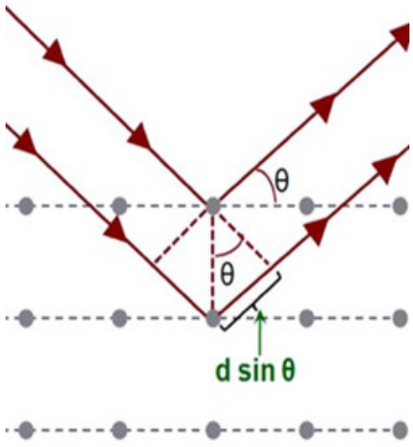

FIGURE 6. Diffraction of x-ray by grain atoms. Adapted from (Macrander. and Huang 2017).

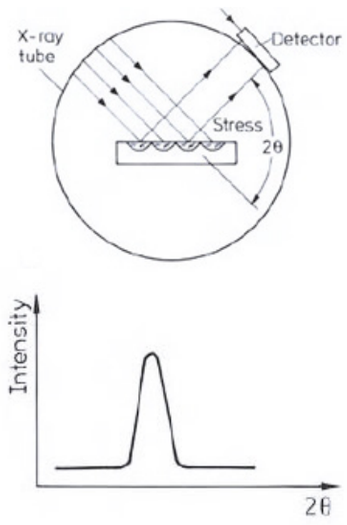

FIGURE 7. Diffraction of x-ray beam over sample surface. Adapted from (Noyan and Cohen 2013)

velocity. Consequently, leads to energy and wave length which they can be calculated by equation (3). Neutrons beam can penetrate bulk samples in comparison with x-rays that used for thin surface condition (Withers and Bhadeshia 2001). Additionally, this technique has the ability to measure RS of weldments at various angles. Additionally, strain can be measured in three different components relative to weldemnt's surface. These components are measured, along the longitudinal (L), transverse (T) and in normal (N) directions. Zhang et al. (2015) have conducted FSW process on 17 vol. % SiCp with AA 2009-T4 composite plates in order to investigate macroscopic and microscopic residual stresses. Strain components were measured as shown in Figure 8 using (STRESS-SPEC) diffractometer. Neutron diffraction method has contributed to investigate the residual stresses in this metal matrix composite (MMC) plate. Therefore, raw diffraction data were evaluated via Stress Texture Calculator (SteCa) software. Results have revealed that the maximum total RS in the MMC at 1500 rpm have reached to 69% of the yield strength of AA 2009-T4 alloy. High rotation speed has small effects on the basic-profiles of the total RS, apart from cumulative in the width of the profiles. Furthermore, increasing the rotation speed induced higher stress in the L direction of the total RS in the MMC, while the lowest value of the N component of the total residual stress in the matrix decreases.Reynolds et al. (2003) reported the effect of welding parameters on the formation residual stresses across FSWed SS 304L joint. The experiment was conducted at single welding speed and two various rotation speeds. It was observed from neutron diffraction results at angle of 90° that the value of the LRS is restricted by the base metal (BM) yield strength for both 300 and 500 rpm rotation speeds Mathon et al. (2009) performed FSW process on PM 2000 steel plate reinforced by oxide dispersion ODS. Neutron diffraction technique detected RS across different welding regions. High asymmetric tensile peaks or RS were observed in TMAZ, thus LRS value reached up to 450 MPa in the advancing side and 320 MPa in retreating side.

OTHER NON-DESTRUCTIVE METHODS

These types of nondestructive methods are based on investigating physical phenomena such as, electromagnetic filed and optical textures of material. The popular techniques that lying under this category are as follow;

ULTRASONIC TECHNIQUE

Ultrasonic method also known as refracted longitudinal (LCR) wave techniques plays a major role in welding inspection field. After welding of isotropic materials elastic waves are propagate at different regions of weld joint (Qozam. 2010).wave are described by their propagation velocity within material as illustrated in Figure 9. The longitudinal mode and dependency of velocity are expressed by equation (4) as;

$$\frac{dV_{11}}{V_{11}} = A_{11} d\varepsilon = \frac{A_{11}}{E} d\sigma \; with \; \varepsilon = \frac{\sigma}{E} \tag{4}$$

Where, E is modulus of elasticity, is the elastic strain, σ is stress, V is wave velocity and A denotes for acoustoelastic constant. However, this method is described clearly in (Bray 2000). Shen et al. (2010) have applied FSW on aluminum 2219-T6 thick plate in order to study the relationship between FSW welding parameters and defects within the butt joint. The obtained results lead to a conclusion of Ultrasonic –scan testing can do well at porosity and tiny voids detecting for FSW joints. Nonetheless, (Tabatabaeipour et al. 2016) have used an immersed ultrasonic method to inspect the root flaws at the bottom of butt-joint of AlZnMgCu (7XXX series) alloy. The alloy has been welded by FSW process on five samples under various welding parameters such as; rotation speed and welding speed. The projected FSW examination was built on an oblique incidence ultrasonic c-scan measurement of back-scatter mode. The results of c-scan backscatter contour image showed at 3.5MHz the formation of Kissing-Bonds Cracks, Lack of Penetration (LOP) defects and distributed worm- hole defect have been effectively identified.

BARKHAUSEN NOISE TECHNIQUE

Barkhausen Noise technique also known as Magnetic Barkhausen Noise (MBN) applies magnetizing force that causes a sudden change in the material's domain; therefore, this tool uses magnetic fields that vary-with-time to determine special features about ferromagnetic materials and it is used to measure the surface residual stresses in the industrial field (Willcox and Mysak 2004). Raja et al. (2018) have analyzed the captured signal induced from FSWed of Steel plates (IS-2062 grade) at range of (70–120) KHz. The inspection process is demonstrated in Figure 10.

NDM METHODS SUMMARY

Summary of NDM of friction stir welding process are listed in Table 2.

SEMI-DESTRUCTIVE (SDM) & DESTRUCTIVE METHODS (DM)

These type of inspection methods are also known as "mechanical approach", are depending on inferring the unique stresses from the displacement incurred by using completely or partially relieving stresses by means of casting off cloth. These techniques rely upon the dimension of deformations because of the relaxation of residual stresses upon elimination of material from the work-piece (Rossini et al. 2012).

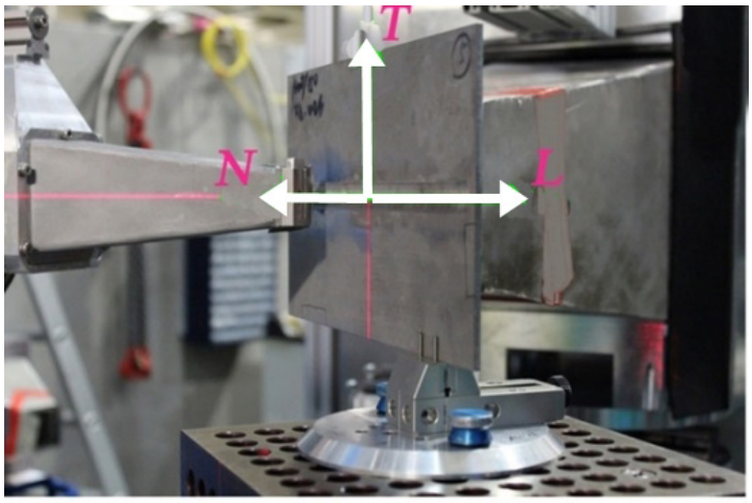

FIGURE 8.Strain measurement component (Zhang et al. 2015)

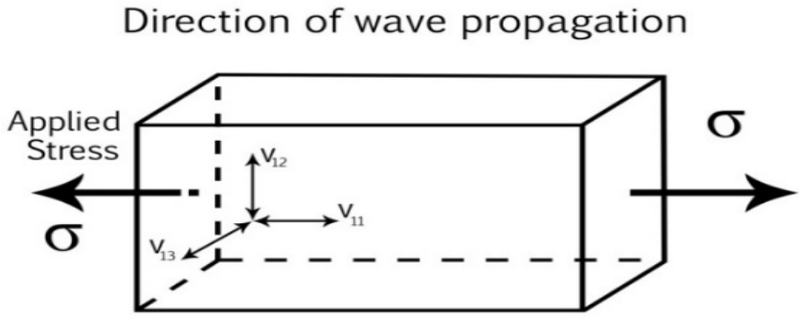

FIGURE 9.Propagation of acoustic waves in a solid.Adapted from (Qozam et al 2010)

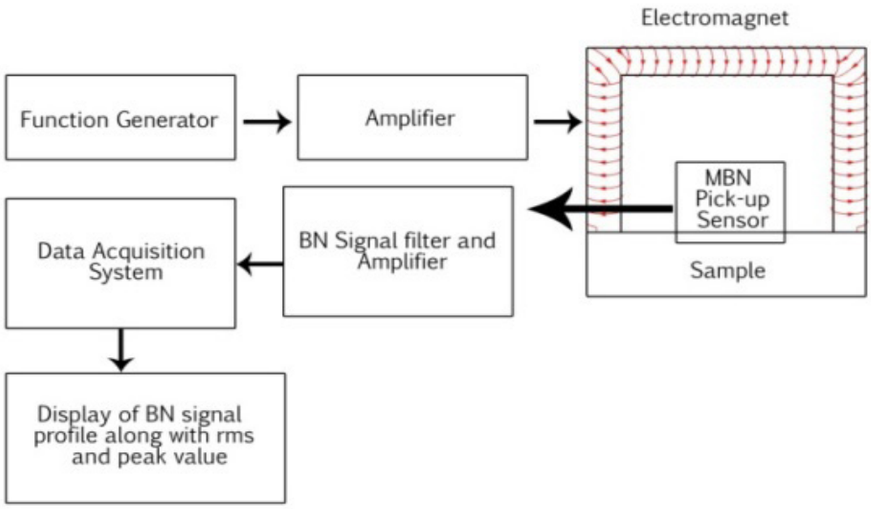

FIGURE 10. Principle of Barkhausen noise analyzer.Adapted from (Raja et al. 2018)

TABLE 2. Recent research on various non-destructive testing methods for FSW process

NDM Type	NDM Parameters	FSW Parameters	FSW Tool material	Plate Material	Plate Dimension (mm)	Author
X-ray Diffraction	-	• Tilt angle 2.5° • 1200 rpm • 25mm/min	H13 steel	AA 1050 aluminum	150×50×4	Mokabberi et al. (2018)
	•20 °to 80 ° •0.1°step size	• 1100 rpm • 1400 rpm • 1600 rpm • 1800 rpm • 16 mm/min • 25 mm/min • 40mm/min	H13 steel	AZ91Mg alloy with AA6063 alloy	100 ×50 ×4	Prasad et al. (2018)
	-	•Tilt angle 2° •1000 rpm •120 mm/min	HSS	ZE41A Mg alloy	4 ×30 width	Carloneand Palazzo (2015)
	•λ = 0.228975 nm Å	•1000 rpm •200 mm/min •F = 6.5-8.5kN	-	AZ31 Mg alloy	175 × 25	Commin et al. (2012)
Ultrasonic C-scan in backscatter mode (pitch catch)	•3.5 MHz •13 mm nominal element size •pulser/Receiverat400V	•Tilt angle 0° •300 rpm •500 rpm •600 rpm	-	AlZnMgCu (7XXX series)	6 mm, thick	Tabatabaei (2016)
Ultrasonic C-Scan	•10–30 MHz •scan velocity: 100 m/s •step length: 0.3 mm	•210 rpm •300 rpm •80 mm/min •150 mm/min	-	2219-T6 aluminum	17–20, thick	Shen, and Hu (2011)
Neutron Diffraction	•λ = 1.64A°	•200 rpm •70 mm/min •90 mm/min •120 mm/min •F = 25kN	PCBN Q70 Grade	MA956 ODS steel	10 mm, thick	Dawson et al. (2017)
	•λ = 1.7458Å •2θ, 91° •2θ, 83°	•600 rpm •1500 rpm	cermet	17vol.%SiCp/2009AA-T4	300×75×3.1	Zhang, et al. (2015)
	•λ = 2.87 Å •2θ, 90°	•600 rpm •50 mm/min •F = 14 kN	PCBN	PM2000	1.3 mm, thick	Mathon et al. (2009)
	•λ = 1.52 Å •90°	•300 rpm •500 rpm •1.7 mm/min •F = 31 kN	WC	SS 304L	305 × 102 × 3.2	Reynolds et al. (2003)
Barkhausen noise-μscan/ Rollscan-300	•70–120 KHz •Sinusoidal 125 Hz	•Tilt angle 2° •550 rpm •600 rpm •700 rpm •150 mm/min	WC	(IS-2062 grade) steel	250×75×3	Raja et al. (2018)

HOLE-DRILLING TECHNIQUE

This semi-destructive technique is used to measure the residual stresses propagated in the welded joints after welding process is conducted (Puymbroeck et al. 2018). The Hole-drilling techniques work principle is based on drilling a relatively small hole about (2 mm deep) on the top of the weldment's surface to relieve to locked stresses into material as shown in Figure 11, at the same time a strain gage is fixed near to the drilled hole in order to measure strain deviation of surface (Schajerand Whitehead 2018). Lim et al (2018) reported the effect of RS on the FSWed SS 409L alloy. Using hole-drilling technique, a 2 mm diameter hole was drilled on the weldment surface near to welding region. Strain gage was used to measure the value of electrical resistance if the relieved residual stresses. Consequently, the peak RS was observed at SZ due to emerging of dynamic recrystallization in this region. Additionally, compressive RS was detected at SZ and TMAZ. However, stresses formed at SZ and TMAZ have improved the mechanical properties of joint. Castro et al. (2011) have measured the residual stresses of a T-joint of

Friction stir welded sheet of AA7075 alloy. The measuring of the residual stress has been achieved by performing 18 altered points adjusted on the root of the advancing side of sheet. The maximum value of residual stress was 100 MPa, located in a distance of 10 mm from the welding line. Stefanescu et al. (2006) measured the residual stresses near the surface of aluminum alloy sheet. The Incremental Centre-hole drilling (ICHD) have been applied, duo its low-cost, many-sided and quick implementation. The results obtained by strain gage rosette (SGR) were analyzed by (invoked Schajer) cumulative program (Stefanescu et al. 2006) validated by comparing empirical results with finite element analysis FEA results, where authors have claimed improvements in ICHD measuring technique at depth range of 10μm to 1 mm.

RING-CORE (RC) TECHNIQUE

This is similar to hole-drilling technique. However, this method involves cutting an annular groove into an object surface as illustrated in Figure 12 where Z stands for depth. Material removed due to annular grooving will relief stresses below weldment surface (stress relaxation) and the critical core is measured at predetermined intensity increments utilizing strain gauge rosette (SGR) or optical methods. The surface stress rest is then decomposed into residual stresses for each depth increment by the usage of numerically decided impact coefficients (from FEA). Generally, depths are constrained to 5mm for a well-known 14mm diameter core, but the use of different stress gauges and groove geometries will allow modifications in total size depth. inside the past the RC technique become especially used to measure 'uniform' pressure profiles to an intensity of 5mm or less, but with latest improvements in analysis methods and the development of a center elimination procedure these depths were prolonged to 25mm (Ajovalasit 1996).

DEEP-HOLE DRILLING TECHNIQUE

This method is based on drilling a reference hole via the component as illustrated in Figure 13. Accurate measuring of the initial diameter is conducted before and after stress launch through trepanning coaxially round it. The variations between the measured diameters before and after stress launch allow the unique residual stresses to be calculated using elasticity deviation, thus the technique is used to measure bi-axial residual stresses appearing within the plane at 90° to the reference of the drilled hole axis (Rossini et al. 2012).

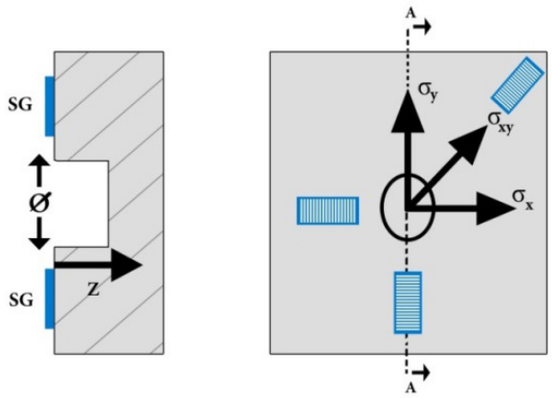

FIGURE 11.Hole-drilling technique with SGR principle. Adapted from (Olabi et al. 2014)

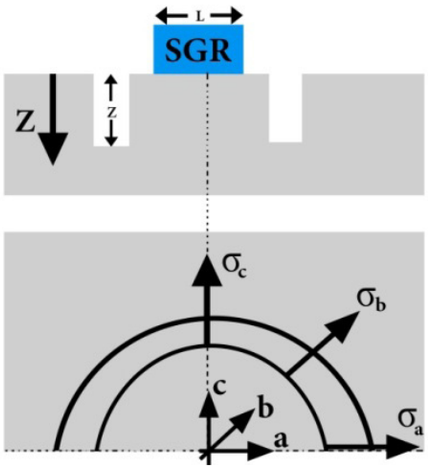

FIGURE 12.Schematic of Ring-core technique.Adapted from (Šarga and Menda 2013)

CONTOUR TECHNIQUE

Contour technique is a novel residual stress measuring technique, first suggested in 2000, it can measure the residual stresses map in 2D perpendicular to the cut surface (Zhang et al. 2005). This technique poses three steps; cutting of weldment, processing the cut surface and analysis of stress. Based on elastic superposition principle, where assuming that material behaves elastically during cutting process. Additionally by assuming that cutting process does not add additional stresses to the plane of interest the process start with cutting the part into two parts as illustrated in Figure 14, and then, the cut surface profiles are measured and processed. After calculating the 'force back', utilizing Finite Element Analysis; the data are mapped in order to observe the initial stress distribution across the plane of interest (prime et al.2002).Sonne et al. (2017) utilized the Contour and FEA to measure residual stresses formed in the FSWed 2024-T3 aluminum alloy. Author claimed that contour technique has attributed in evaluating RS by comparison empirical results with FEA data. High peak stresses were observed at mid-section of welded plate by 2D mapping. However, Trummer et al (2011) have used contour technique in order to measure perpendicular RS to the FSWed AA 6082-T6 alloy surface. Utilizing (CATIM – Porto) Approx. 2000 point of the cut surface were measured. The measured data were exported to MATLAB-FEM package in order to analyze and finalize the 2D surface mesh of the cut surface. Results as shown in Figure 15; display the distribution of RS at SZ of FSWed plate.

Prime et al. (2006) utilized contour technique on dissimilar aluminum alloys of 7050-T7451 and 2024-T351 joint butt joined by FSW process. After EDM wire cutting process is conducted; FEA model was created utilizing 18,900 bi-quadratic (20 node) with hexahedral elements shape.Low residual stresses were detected within aluminum plates. Furthermore, the peak stresses of around 43 MPa but, less than 20% of the material flow stress point was also detected.

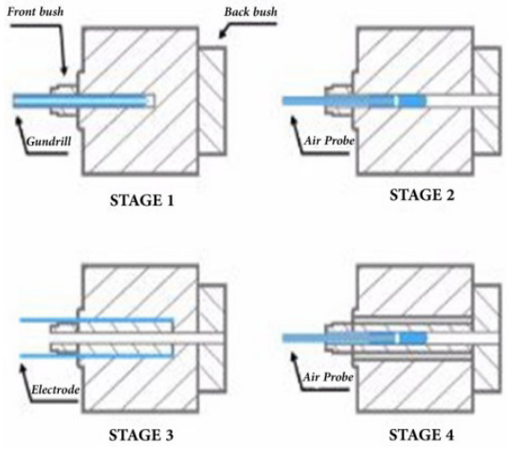

FIGURE 13.Schematic of the four Deep-Hole drilling stages.Adapted from Mahmoudi (2009)

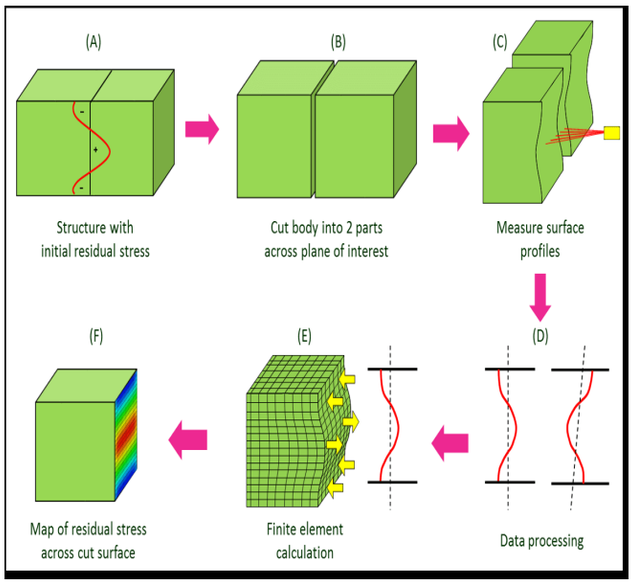

FIGURE 14. Contour technique process (Prim et al. 2002)

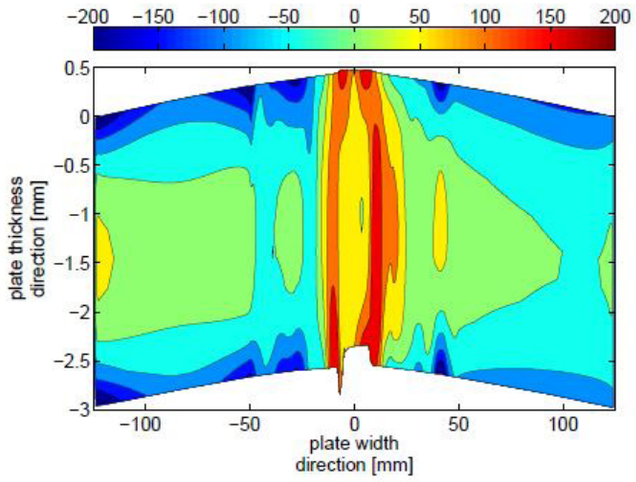

FIGURE 15. RS distribution in SZ obtained by contour method (Sonne et al. 2017)

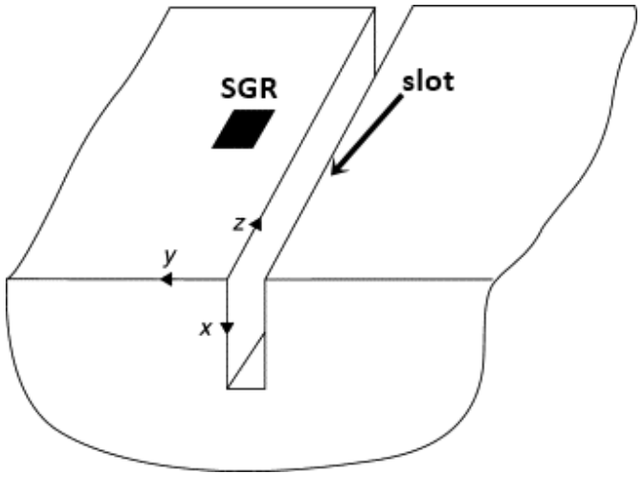

FIGURE 16. Schematic of slitting technique. Reproduced From (Cheng and Finnie 2007)

SLITTING TECHNIQUE

Slitting or sectioning method as illustrated schematically in Figure 16 thus, it is based on reducing a slit across a work's surface, generally cutting process is implemented using wire-EDM, and measuring the surfaces strains with SG placed near to the slit. At some point of the process, the slit depth is extended incrementally to predetermined depths and the strain at each depth increment is recorded. Evaluation of the strain records from the Slitting system is achieved by use of elastic-inverse solution (Cheng and Finnie 2007). Deplus et al. (2011) have performed Slitting technique on 2024-T3, 6082-T6 and 5754-H111 FSWed aluminum alloys. A slit cut is made on the surface of the welded plates performed by wire electric discharge which relive stresses from the weldment, and strain was measured by using SG (EA-13-062AQ-350/LE). Mapping Result showed distributed RS with a plateau shape formed across 5754-H111 weld center. However, 'M-shape' RS were observed into weld centers of 2024-T3 and 6082-T6 alloys. Sonne et al. (2013) have compared hot and cold FSWed 2024-T3 aluminum alloy under different welding parameters in order to investigate the effect of (Hardening-Law) on RS and yield stress. ABAQUS software was used to simulate the built-in metallurgical 'softening model' based on the 'Thermal Pseudo Mechanical' (TPM) model for heat generation. Cold FSW have reduced the value of yield strength of the welded part. However, the RS was not affected. Hot FSW process also decreased the yield stress value. RS induced by hot FSW was affected due to excessive metal softening near the weld center line.

SDM AND DM SUMMARY

Table 3 highlights recent researches on SDM & DM with FSW process.

PARAMETERS OPRIMIZATION

It is well know that for several welding methods, the key challenge for many manufacturers is to select the suitable welding process parameters that will produce a high quality welded joint (Cole at al. 2014). Optimizing of friction stir

TABLE 3. Recent research on SDM and DM testing of FSW process

SDM\DM Technique	SDM\DM Parameters	FSW Parameters	FSW Tool Material	Plate Material	Plate Dimension (mm)	Author
Hole- drilling	1.hole 2 mm Ø	1. 800 rpm 2. 250 mm/min	PCBN	SS SUS 409L	400 × 150 × 2	Lim et al. (2018)
	1.18 points at welding root	• null tilt angle • 1120 rpm • 200 mm/min • F = 7000 to 7500 N • dwell time = 8 s.	-	AA 6056-T4 with AA 7075-T6	3.3	Castro et al. (2011)
	1.rz/rm = 0.4 2.12000 rpm 3.1.4µm/sec	-	-	Spring-Steel with Aluminum Titanium	100×100×24 85×85×14 30×20×25	Stefanescu et al. (2006)
Contour	-	8. Tilt angle 2° 9. 1400 rpm 10. 70 mm/min	AISI1040	AA 2024-T3	200×30×4	Sonne et al. (2017)
	24 mm'min, cutting speed	11. 1500 rpm 12. 290 mm/min	-	AA 6082-T6	180 × 3 126 × 3	Trummer at el. (2011)
	-	13. 50.8 mm/min	-	AA 7050-T7451 with AA 2024T351	54 × 25.4	Prime et al. (2006)
Slitting	-	14. 400 rpm 15. 100 mm/min	-	AA 2024-T3	3.175	Sonne et al. (2013)
	-	16. 1000 rpm 17. 350 mm/min hot 18. 1100 mm/min cold	-	AA 2024-T3 AA 6082-T6	4	Deplus et al. (2011)

welding parameters is a crucial concern in order to anticipate process characteristics and to obtain the best output. Thus, methods such as; analysis of variance (ANOVA), Taguchi and Response Surface Methodology (RSM) are distinguished and reliable techniques for such case (Panneerselvam and Lenin 2015). Kasman and Yenier (2014) employed ANOVA technique to study the effect of the varied parameters on FSWed AA 5754/AA 7075 alloys. The butt-welded joint was identified by UTS, hardness and elongation percentage. In addition, regression analysis contributed to construct a mathematical model relating these outputs with FSW parameters. The results obtained from ANOVA show that all the parameters have a significant effect on UTS. Moreover, the influencers are 41.41 % for welding speed, 17.58 % for shoulder diameter, and 13.28 % for rotation speed. For AA 6061-T6/AA 7075-T6 alloys, (Tamjidy et al. 2017) have utilized ANOVA to investigate similar scopes of study in (Kasman and Yenier 2014). This multi response optimization problem has been solved by multi-objective biogeography based optimization (MOBBO). The results showed that this algorithm in combination with the mathematical regression model is an advantageous manner to optimize the FSW process parameters to obtain the best mechanical properties of the FSWed joints. Experimental values of UTS, elongation and hardness are 252.23 MPa, 8.19% and 72.11 HV were optimized at welding parameters of tilt angle of 1.92°, welding speed of 149.73 mm/min and tool offset of -074 mm respectively. Pradeep and Muthukumaran (2013) carried out an experimental investigation to study the effect of FSW parameters, namely, rotation speed, welding speed and tilt angle on the mechanical properties of joint. Taguchi's L_9 orthogonal array technique has been used to optimize the process parameters. FSWed (IS: 3039 grade II steel alloy) butt-joint was produced successfully. The effect of the combination of the input functions as a result is produced by the signal to noise (S/N) ratio and mean response. The most significant parameter on UTS, with a percentage tilt angle of 63.46%, followed by the welding speed of 32.83% and rotation speed of 2.81%. Bayazida et al. (2015) predicted FSW process parameters via Taguchi method. S/N analysis detected that UTS reached to maximum value when, welding speed of 120 mm/min and rotation speed of1600 rpm for AA 6063/AA 7075 alloys. Elatharasan and Kumar (2013) developed a mathematical model via RSM method utilizing three input parameters (rotation speed, welding speed and axial force) corresponding with three responses (UTS, yield strength and %elongation). The material AA 6061-T6 has been welded by FSW process. A maximum UTS of 197.50 MPa, Yield strength of 175.25MPa and % of elongation of 6.96 with the optimized parameters of 1199 rpm rotational speed, 30 mm/min welding speed and 9.0 kN axial force.

CONCLUSION

Based on the reviewed articles, the key findings can by drawn as;

1. Residual stresses are unavoidable and formed nearly at each step of (heat-treatment, cold working and welding) processes.

2. Compressive residual stresses induced by shot peening processcan contribute to restrict and limit crack propagation.
3. X-ray technique is extensively applied in measuring residual stresses of FSW processes at different angles.
4. Neutron diffraction technique is capable to measure residual stresses at greater depth than x-ray without interacting with material or harming weld surface.
5. Barkhausen Noise technique are not extensively used in quality control of the FSW process due to its restriction to ferromagnetic matrials.However, ultrasonic technique was used vastly on FSW due to its applicability for most metals.
6. Semi destructive and destructive techniques have nearly similar measuring mechanism in terms of material removing and strain measuring processes.
7. Deep-hole drilling technique has not been applied in FSW process quality assessment,may be due its excessive hole depth; where in FSW only near surface residual stresses are need to be inspected.
8. ANOVA, Taguchi and RSM techniques proved their reliability in optimizing the best FSW parameters with maximum mechanical properties.

DECLARATION OF COMPETING INTEREST

None.

REFERENCES

Ajovalasit, A., Petrucci, G., & Zuccarello, B. 1996. Determination of nonuniform residual stresses using the ring-core method. *Journal of Engineering Materials and Technology* 118(2): 224-228.

Al-Moussawi, M., & Smith, A. J. 2018. Defects in friction stir welding of steel. *Metallography, Microstructure, and Analysis*: 1-9.

Barsoum, Z., Samuelsson, J., Jonsson, B., & Björkblad, A. 2012. Fatigue design of lightweight welded vehicle structures: Influence of material and production procedures. *Proceedings of the Institution of Mechanical Engineers, Part B: Journal of Engineering Manufacture* 226(10): 1736-1744.

Bayazid, S. M., Farhangi, H. & Ghahramani, A. 2015. Investigation of friction stir welding parameters of 6063-7075 aluminum alloys by Taguchi method. *Procedia Materials Science* 11: 6-11.

Bray, D. E. 2000. Current directions of ultrasonic stress measurement techniques. In *15th world conference on non-destructive testing*.

Büyüköztürk, O., & Taşdemir, M. A. 2012. *Nondestructive Testing of Materials and Structures* (Vol. 6). Springer Science & Business Media.

Carlone, P., & Palazzo, G. S. 2015. Characterization of TIG and FSW weldings in cast ZE41A magnesium alloy. *Journal of Materials Processing Technology* 215: 87-94.

Castro, R. A. S., Richter-Trummer, V., Tavares, S. M. O., Moreira, P. M. G. P., Vilaça, P., & de Castro, P. M. S. T. 2011. Friction stir welding on t-joints: Residual stress evaluation. *Revista da Associação Portuguesa de Análise Experimental de Tensões* ISSN, 1646, 7078.

Chang, F. K. 1999. *Structural Health Monitoring 2000*. CRC Press.

Chen, X. G., Da Silva, M., Gougeon, P., & St-Georges, L. 2009. Microstructure and mechanical properties of friction stir welded AA6063–B4C metal matrix composites. *Materials Science and Engineering: A* 518(1-2): 174-184.

Cheng, W., & Finnie, I. 2007. *Residual Stress Measurement and the Slitting Method*. Springer Science & Business Media.

Cole, E. G., Fehrenbacher, A., Duffie, N. A., Zinn, M. R., Pfefferkorn, F. E., & Ferrier, N. J. 2014. Weld temperature effects during friction stir welding of dissimilar aluminum alloys 6061-t6 and 7075-t6. *The International Journal of Advanced Manufacturing Technology* 71(1-4): 643-652.

Cole, H. 1970. Bragg's law and energy sensitive detectors. *Journal of Applied Crystallography* 3(5): 405-406.

Commin, L., Dumont, M., Rotinat, R., Pierron, F., Masse, J. E., & Barrallier, L. 2012. Influence of the microstructural changes and induced residual stresses on tensile properties of wrought magnesium alloy friction stir welds. *Materials Science and Engineering: A* 551: 288-292.

Dawson, H., Serrano, M., Cater, S., Wady, P., Pirling, T., & Jimenez-Melero, E. 2017. Residual stress distribution in friction stir welded ODS steel measured by neutron diffraction. *Journal of Materials Processing Technology* 246: 305-312.

Deplus, K., Simar, A., Van Haver, W., & De Meester, B. 2011. Residual stresses in aluminium alloy friction stir welds. *The International Journal of Advanced Manufacturing Technology* 56(5-8): 493-504.

Ding, R. J. 2008. Friction Stir Welding: Standards and Specifications in Today's US Manufacturing and Fabrication.

Dressler, U., Biallas, G. & Mercado, U. A. 2009. Friction stir welding of titanium alloy TiAl6V4 to aluminium alloy AA2024-T3. *Materials Science and Engineering: A* 526(1-2): 113-117.

Elatharasan, G., & Kumar, V. S. 2013. An experimental analysis and optimization of process parameter on friction stir welding of AA 6061-T6 aluminum alloy using RSM. *Procedia Engineering* 64: 1227-1234.

Hutchings, M. T., Withers, P. J., Holden, T. M. & Lorentzen, T. 2005. *Introduction to the Characterization of Residual Stress by Neutron Diffraction*. CRC press.

Kaniowski, J., Korzeniewski, B., & Hakanen, M. 2011. Methodology of residual stress

Kasman, Ş. & Yenier, Z. 2014. Analyzing dissimilar friction stir welding of AA5754/AA7075. *The International Journal of Advanced Manufacturing Technology* 70(1-4): 145-156.

Lim, Y. S., Kim, S. H., & Lee, K. J. 2018. Effect of residual stress on the mechanical properties of FSW Joints with SUS409L. *Advances in Materials Science and Engineering*, *2018*.

Macherauch, E. 1987. Origin, measurement and evaluation of residual stresses. Residual stresses in science and technology. In Papers presented at the Int. Conf. on residual stresses, 1986 Garmisch-Partenkirchen (pp. 3-26).

Macherauch, E. & Wohlfahrt, H. 1978. Different sources of residual stress as a result of welding. In Proc. Conf. on Residual Stresses in Welded Construction and Their Effects, 1978, 267-282.

Macrander, A. T. & Huang, X. 2017. Synchrotron x-ray optics. *Annual Review of Materials Research* 47: 135-152.

Mahmoudi, A. H., Hossain, S., Truman, C. E., Smith, D. J. & Pavier, M. J. 2009. A new procedure to measure near yield residual stresses using the deep hole drilling technique. *Experimental Mechanics* 49(4): 595-604.

Mathon, M. H., Klosek, V., De Carlan, Y. & Forest, L. 2009. Study of PM2000 microstructure evolution following FSW process. *Journal of Nuclear Materials* 386: 475-478.

Mokabberi, S. R., Movahedi, M. & Kokabi, A. H. 2018. Effect of interlayers on softening of aluminum friction stir welds. *Materials Science and Engineering: A*.

Noyan, I. C., & Cohen, J. B. 2013. *Residual Stress: Measurement by Diffraction and Interpretation*. Springer.

Olabi, A. G., Lorza, R. L. & Benyounis, K. Y. 2014. Quality control in welding process.

Panneerselvam, K., & Lenin, K. 2015. Parameters optimization in FSW of polypropylene based on RSM. *Multidiscipline Modeling in Materials and Structures* 11(1): 32-42.

Pope, C. G. 1997. X-ray diffraction and the Bragg equation. *Journal of Chemical Education* 74(1): 129.

Pradeep, A. & Muthukumaran, S. 2013. An analysis to optimize the process parameters of friction stir welded low alloy steel plates. *International Journal of Engineering, Science and Technology* 5(3): 25-35.

Prasad, B. L., Neelaiah, G., Krishna, M. G., Ramana, S. V. V., Prakash, K. S., Sarika, G. & Sunil, B. R. 2018. Joining of AZ91 Mg alloy and Al6063 alloy sheets by friction stir welding. *Journal of Magnesium and Alloys*.

Prime, M. B., Gnäupel-Herold, T., Baumann, J. A., Lederich, R. J., Bowden, D. M. & Sebring, R. J. 2006. Residual stress measurements in a thick, dissimilar aluminum alloy friction stir weld. *Actamaterialia* 54(15): 4013-4021.

Prime, M. B., Hill, M. R., DeWald, A. T., Sebring, R. J., Dave, V. R. & Cola, M. J. 2002. Residual stress mapping in welds using the contour method. In *International Conference, April* 15: 19.

Puymbroeck, E. V., Nagy, W., Fang, H. & De Backer, H. 2018. Determination of residual weld stresses with the incremental hole-drilling method in tubular steel bridge joints. *Procedia Engineering* 213: 651-661.

Qozam, H., Chaki, S., Bourse, G., Robin, C., Walaszek, H. & Bouteille, P. 2010. Microstructure effect on the Lcr elastic wave for welding residual stress measurement. *Experimental Mechanics* 50(2): 179-185.

Raja, A. R., Yusufzai, M. K. &Vashista, M. 2018. Micro-magnetic analysis of friction stir welded steel plates. *The International Journal of Advanced Manufacturing Technology*, 1-9.

Richter-Trummer, V., Moreira, P. M. G. P., Ribeiro, J. & de Castro, P. M. S. T. 2011. The contour method for residual stress determination applied to an AA6082-T6 friction stir butt weld. In *Materials Science Forum* (Vol. 681, pp. 177-181).Trans Tech Publications.

Rossini, N. S., Dassisti, M., Benyounis, K. Y. & Olabi, A. G. 2012. Methods of measuring residual stresses in components. *Materials & Design* 35: 572-588.

Šarga, P., & Menda, F. 2013.Comparison of ring-core method and hole-drilling method used for determining residual stresses. *Am. J. Mech. Eng*. 1(7): 335-338.

Schajer, G. S. & Whitehead, P. S. 2018. Hole-drilling method for measuring residual stresses. *Synthesis SEM Lectures on Experimental Mechanics* 1(1): 1-186.

Sidhu, M. S. & Chatha, S. S. 2012. Friction stir welding–process and its variables: A review. *International Journal of Emerging Technology and Advanced Engineering* 2(12): 275-279.

Singh, B. 2012. *A Hand Book on Friction Stir Welding*. 1st edition. UK: LAP Lambert Academic Publishing.

Sonne, M. R., Carlone, P. & Hattel, J. H. 2017. Assessment of the contour method for 2-D cross sectional residual stress measurements of friction stir welded parts of AA2024-T3—*Numerical and Experimental Comparison. Metals* 7(11): 508.

Sonne, M. R., Tutum, C. C., Hattel, J. H., Simar, A. & De Meester, B. 2013. The effect of hardening laws and thermal softening on modeling residual stresses in FSW of aluminum alloy 2024-T3. *Journal of Materials Processing Technology* 213(3): 477-486.

Stefanescu, D., Truman, C. E., Smith, D. J. & Whitehead, P. S. 2006. Improvements in residual stress measurement by the incremental centre hole drilling technique. *Experimental Mechanics* 46(4): 417.

Stenberg, T., Barsoum, Z., Åstrand, E., Öberg, A. E., Schneider, C. & Hedegård, J. 2017. Quality control and assurance in fabrication of welded structures subjected to fatigue loading. *Welding in the World* 61(5): 1003-1015.

Suominen, L., Khurshid, M. & Parantainen, J. 2013. Residual stresses in welded components following post-weld treatment methods. *Procedia Engineering* 66: 181-191.

Tabatabaeipour, M., Hettler, J., Delrue, S. & Van Den Abeele, K. 2016. Non-destructive ultrasonic examination of root defects in friction stir welded butt-joints. *NDT & E International* 80: 23-34.

Tamjidy, M., Baharudin, B. T. H. T., Paslar, S., Matori, K., Sulaiman, S. & Fadaeifard, F. 2017. Multi-objective optimization of friction stir welding process parameters of AA6061-T6 and AA7075-T6 using a biogeography based optimization algorithm. *Materials* 10(5): 533.

Thomas, W. M., Johnson, K. I. & Wiesner, C. S. 2003. Friction stir welding–recent developments in tool and process technologies. *Advanced Engineering Materials* 5(7): 485-490.

Thomas, W. M., Wiesner, C. S., Marks, D. J. & Staines, D. G. 2009. Conventional and bobbin friction stir welding of 12% chromium alloy steel using composite refractory tool materials. *Science and Technology of welding and Joining* 14(3): 247-253.

Uzun, H. 2007. Friction stir welding of SiC particulate reinforced AA2124 aluminium alloy matrix composite. *Materials & Design* 28(5): 1440-1446.

Wei, L. Y. & Nelson, T. W. 2011. Correlation of microstructures and process variables in FSW HSLA-65 steel. *Welding Journal* 90(1–3): 95s-101s.

Willcox, M. & Mysak, T. 2004. *An Introduction to Barkhausen Noise and Its Applications*. Herefordshire: Insight NDT Publication.

Withers, P. J. & Bhadeshia, H. K. D. H. 2001. Residual stress. Part 2–Nature and origins. *Materials Science and Technology* 17(4): 366-375.

Withers, P. J. & Bhadeshia, H. K. D. H. 2001. Residual stress. Part 1–measurement techniques. *Materials Science and Technology* 17(4): 355-365.

Zhang, X. X., Ni, D. R., Xiao, B. L., Andrä, H., Gan, W. M., Hofmann, M. & Ma, Z. Y. 2015. Determination of macroscopic and microscopic residual stresses in friction stir welded metal matrix composites via neutron diffraction. *Acta Materialia* 87: 161-173.

Zhang, Y., Pratihar, S., Fitzpatrick, M. E. & Edwards, L. 2005. Residual stress mapping in welds using the contour method. In Materialsscience forum (Vol. 490, pp. 294-299).Trans Tech Publications.